$BaZn_2(HAs_2O_7)AsO_4$: A Novel Barium Zinc Arsenate Containing Zn_4O_{16} Clusters and Hydrogen Diarsenate Groups

Nei-Yih Fan and Sue-Lein Wang*

Department of Chemistry, National Tsing Hua University, Hsinchu, Taiwan 30043

Received December 28, 1995[⊗]

A novel barium zinc arsenate has been synthesized under hydrothermal conditions and characterized by single-crystal X-ray diffraction, IR spectroscopy, and thermogravimetric analysis. Being the first compound in the Ba−Zn−As^V−O system, the structure contains tetramers of ZnO_5 square pyramids which have not been seen in the Zn/X/O lattices, where X = P or As. Diffraction measurements were performed on a CCD area detector system. Crystal data: $BaZn_2(HAs_2O_7)AsO_4$, monoclinic, $P2_1/c$, $a = 11.5773(3)$ Å, $b = 8.0975(2)$ Å, $c = 10.0511(3)$ Å, $\beta = 93.862(2)°$, $Z = 4$. The framework consists of Zn_4O_{16} cluster units, AsO_4 tetrahedra, and HAs_2O_7 groups. The cluster units, each formed by four ZnO_5 pyramids sharing alternate corners and edges, are cross-linked by AsO_4 tetrahedra to form an infinite sheet $^2_\infty[Zn_2AsO_4]$. The sheets are held together via HAs_2O_7 groups to form a three-dimensional network. Barium cations are located in the cavities surrounded by HAs_2O_7 anions. $BaZn_2(HAs_2O_7)AsO_4$ is the first structurally characterized compound which contains the hydrogen diarsenate group, $HAs_2O_7^{2-}$.

Introduction

Recent investigation of transition metal arsenates in the A−M−As^V−O systems, where A = alkali-metal, alkaline-earth-metal, and organic cations and M = V, Fe, Co, and Cu, has revealed many new compounds with complex polyhedral connections,[1,2] which are often different from those of transition metal phosphates. To explore novel frameworks built up from various polyhedra, we have extended our work to zinc-based arsenate systems. A great number of ternary and quaternary zinc phosphates are known, and many of these structures are complex due to the various coordination geometries adopted by ZnO_x (x = 4, 5, 6).[3] Like other transition metal-based phosphates, zinc−oxygen polyhedra may be linked into finite cluster units or infinite 1-D chains or 2-D layers. Surprisingly, cluster units containing only ZnO_5 square pyramids in the structures of either phosphates or arsenates are rare as compared to those with linked ZnO_4 tetrahedra, ZnO_5 trigonal bipyramids, ZnO_6 octahedra, or Zn−O polyhedra with mixed coordination geometries.[4] α-$CaZn_2(PO_4)_2$,[5] $Zn_2VO(PO_4)_2$,[6] and $ZnCu(AsO_4)_2$[7] are the only known examples which contain cluster units of ZnO_5 square pyramids. All of these three compounds contain edge-sharing dimers of ZnO_5 square pyramids.

Relative to the rich structural chemistry of zinc phosphates, little is known about the structural chemistry of zinc arsenates. By employing hydrothermal reactions, we have obtained the new compound $BaZn_2(HAs_2O_7)AsO_4$, in which tetrameric units of ZnO_5 square pyramids are present. Furthermore, it contains the hydrogen diarsenate anion, $HAs_2O_7^{2-}$, which is the first example in condensed phases. There is actually very scant information on the hydrogen diarsenate compounds in the literature. Reported here is the synthesis and crystal structure of the first member in the Ba−Zn−As^V−O system.[8] IR data and thermal decomposition schemes pertaining to the HAs_2O_7 group are presented as well.

Table 1. Crystallographic Data for $BaZn_2(HAs_2O_7)AsO_4$

empirical formula	$HAs_3BaO_{11}Zn_2$
space group	$P2_1/c$
a, Å	11.5773(3)
b, Å	8.0975(2)
c, Å	10.0511(3)
β, deg	93.862(2)
V, Å^3	940.12(7)
Z	4
ρ_{calcd}, g cm^{-3}	4.733
μ, cm^{-1}	197.37
λ, Å	0.710 73
T, °C	23
$R(F_0)^a$	0.0244
$R_w(F_0)^b$	0.0297

[a] $R = \sum||F_0| - |F_c||/\sum|F_0|$. [b] $R_w = [\sum(|F_0| - |F_c|)^2/\sum w|F_0|^2]^{1/2}$, $w = [\sigma^2(F_0) + gF_0^2]^{-1}$, $g = 0.0015$.

[⊗] Abstract published in *Advance ACS Abstracts,* July 1, 1996.

(1) (a) Wang, S. L.; Lee, Y. H. *Inorg. Chem*. **1994**, *33*, 3845. (b) Wang, S. L.; Hsu, K. F.; Nieh, Y. P. *J. Chem. Soc., Dalton Trans*. **1994**, 1681. (c) Wang, S. L.; Horng, J. C.; Lee, Y. H. *J. Chem. Soc., Dalton Trans*. **1994**, 1825. (d) Cheng, C. Y.; Wang, S. L. *J. Chem. Soc., Dalton Trans*. **1992**, 2395. (e) Wang, S. L.; Cheng, C. Y. *J. Solid State Chem*. **1994**, *107*, 277. (f) Wang, S. L.; Hsu, K. F. *J. Chin. Chem. Soc*. **1994**, *41*, 729. (g) Wang, S. L.; Wu, C. H.; Liu, S. N. *J. Solid State Chem*. **1994**, *113*, 37.

(2) (a) Lii, K. H. *Inorg. Chem*. **1995**, *34*, 1700. (b) Haushalter, R. C.; Wang, Z.; Meyer, L. M.; Dhingra, S. S.; Thompson, M. E.; Zubieta, J. *Chem. Mater*. **1994**, *6*, 1463. (c) Masquelier, C.; d'Yvoire, F.; Collin, G. *J. Solid State Chem*. **1995**, *118*, 33.

(3) (a) Durif, P. A.; Averbuch-Pouchot, M. T.; Guitel, J. C. *Acta Crystallogr*. **1975**, *B31*, 2680. (b) Harrison, W. T. A.; Nenoff, T. M.; Gier, T. E.; Stucky, G. D. *J. Solid State Chem*. **1994**, *113*, 168. (c) Keller, P.; Riffel, H.; Hess, H. *Z. Kristallorg*. **1982**, *158*, 33. (d) Harrison, W. T. A.; T. M.; Gier, T. E.; Nicol, J. M.; Stucky, G. D. *J. Solid State Chem*. **1995**, *114*, 249. (e) Harrison, W. T. A.; Nenoff, T. M.; Gier, T. E.; Stucky, G. D. *Inorg. Chem.* **1992**, *31*, 5395. (f) Nenoff, T. M.; Harrison, W. T. A.; Gier, T. E.; Stucky, G. D. *J. Am. Chem. Soc*. **1991**, *113*, 378. (g) Schmidt, R.; Kniep, R. *Z. Kristallogr*. **1991**, *196*, 312. (h) Mundi, L. A.; Haushalter, R. C. *Inorg. Chem.* **1992**, *31*, 3050.

(4) (a) Ortiz-Avila, C. Y.; Sauattrito, P. J.; Shieh, M. H.; Clearfield, A. *Inorg. Chem*. **1989**, *28*, 2608. (b) Tordjman, P. I.; Durif, A.; Averbuch-Pouchot, M. T.; Guitel, J. C. *Acta Crystallogr*. **1975**, *B31*, 1143. (c) Kata, T.; Miura, Y. *Miner. J. Jpn.* **1977**, *8*, 320. (d) Atanasov, M.; Petrov, K.; Mirtcheva, E. *J. Solid State Chem*. **1995**, *118*, 303.

(5) Lii, K. H.; Tsai, H. J. *J. Solid State Chem*. **1991**, *90*, 291.

(6) Jakeman, R. J. B.; Cheetham, A. K. *J. Am. Chem. Soc*. **1988**, *110*, 1140.

(7) Keller, P.; Hess, H.; Dunn, P. J. *Tsch. Miner. Petrograp. Mitte*. **1979**, *26*, 167.

(8) There may be several compouds have been reported in the Ba−Zn−As−O system, but the valence for the As atom is not 5+.

S0020-1669(95)01655-7 CCC: $12.00

Table 2. Atomic Coordinates and Thermal Parameters ($Å^2$) for $BaZn_2(HAs_2O_7)AsO_4$

atom	*x*/*a*	*y*/*b*	*z*/*c*	U_{eq}[a]	atom	*x*/*a*	*y*/*b*	*z*/*c*	U_{eq}[a]
Ba	0.80009(4)	−0.52641(5)	0.50402(4)	0.0125(2)	O(4)	0.9253(4)	−0.5014(6)	0.1041(5)	0.014(1)
Zn(1)	0.70492(7)	−0.18565(9)	0.30709(8)	0.0131(3)	O(5)	1.1268(4)	−0.5841(7)	0.2389(6)	0.024(2)
Zn(2)	0.45242(7)	−0.18689(9)	0.49839(8)	0.0119(3)	O(6)	0.9118(5)	−0.7165(6)	0.3018(5)	0.022(2)
As(1)	0.77480(6)	−0.47387(8)	0.10273(7)	0.0098(2)	O(7)	1.0099(4)	−0.8257(6)	0.0777(5)	0.019(2)
As(2)	1.00389(6)	−0.66709(9)	0.17743(7)	0.0127(2)	O(8)	0.4729(4)	−0.0255(6)	0.3692(5)	0.013(1)
As(3)	0.49271(6)	0.01315(9)	0.20306(7)	0.0091(2)	O(9)	0.6356(4)	−0.0232(6)	0.1872(5)	0.012(1)
O(1)	0.7551(3)	−0.4131(6)	0.2579(5)	0.011(1)	O(10)	0.4108(4)	−0.1321(6)	0.1226(5)	0.015(1)
O(2)	0.7216(4)	−0.6555(6)	0.0513(5)	0.015(1)	O(11)	0.4549(4)	−0.1984(5)	0.1339(5)	0.011(1)
O(3)	0.7505(4)	−0.3179(6)	0.0000(5)	0.016(2)	H	0.9016	−0.8174	0.3048	0.05

[a] U_{eq} is defined as one-third of the trace of the orthorgonalized $\mathbf{U}_{ij}$ tensor.

Table 3. Selected Bond Distances (Å) and Angles (deg) for $BaZn_2(HAs_2O_7)AsO_4$[a]

Ba−O(1)	2.657(5)	Ba−O(6)	2.920(6)	Ba−O(2)[a]	2.783(5)
Ba−O(3)[b]	2.847(5)	Ba−O(9)[b]	2.766(5)	Ba−O(7)[a]	2.764(5)
Ba−O(5)[c]	2.810(5)	Ba−O(7)[d]	2.898(5)	Ba−O(10)[e]	2.810(5)
Zn(1)−O(1)	2.004(5)	Zn(1)−O(3)[b]	1.975(5)	Zn(1)−O(5)[d]	2.193(5)
Zn(1)−O(9)	1.922(5)	Zn(1)−O(11)[e]	2.193(5)	Zn(2)−O(8)[g]	2.018(5)
Zn(2)−O(2)[f]	2.059(5)	Zn(2)−O(8)	2.178(5)	Zn(2)−O(10)[b]	2.005(5)
Zn(2)−O(11)[e]	1.993(5)	As(1)−O(1)	1.666(5)	As(1)−O(2)	1.663(5)
As(1)−O(3)	1.643(5)	As(1)−O(4)	1.756(5)	As(2)−O(4)	1.755(5)
As(2)−O(5)	1.655(5)	As(2)−O(6)	1.743(6)	As(2)−O(7)	1.633(5)
As(3)−O(8)	1.704(5)	As(3)−O(9)	1.698(5)	As(3)−O(10)	1.683(5)
As(3)−O(11)	1.699(5)	O(6)−H	0.83	H···O(5)[h]	2.22

O(1)−Zn(1)−O(3)[b]	101.1(2)	O(2)[f]−Zn(2)−O(8)	84.4(2)
O(1)−Zn(1)−O(5)[d]	90.9(2)	O(2)[f]−Zn(2)−O(8)[g]	116.7(2)
O(1)−Zn(1)−O(9)	126.2(2)	O(2)[f]−Zn(2)−O(10)[b]	88.2(2)
O(1)−Zn(1)−O(11)[e]	86.4(2)	O(2)[f]−Zn(2)−O(11)[e]	117.2(2)
O(3)[b]−Zn(1)−O(5)[d]	91.1(2)	O(8)−Zn(2)−O(8)[g]	79.8(2)
O(3)[b]−Zn(1)−O(11)[e]	85.1(2)	O(8)−Zn(2)−O(11)[e]	83.4(2)
O(3)[b]−Zn(1)−O(9)	132.7(2)	O(8)−Zn(2)−O(10)[b]	171.5(2)
O(5)[d]−Zn(1)−O(9)	87.2(2)	O(8)[g]−Zn(2)−O(11)[e]	121.1(2)
O(5)[d]−Zn(1)−O(11)[e]	174.9(2)	O(8)[g]−Zn(2)−O(10)[b]	100.0(2)
O(9)−Zn(1)−O(11)[e]	97.9(2)	O(10)[b]−Zn(2)−O(11)[e]	103.7(2)
O(1)−As(1)−O(2)	118.8(2)	O(4)−As(2)−O(5)	104.7(3)
O(1)−As(1)−O(3)	109.4(2)	O(4)−As(2)−O(6)	98.7(2)
O(1)−As(1)−O(4)	103.2(2)	O(4)−As(2)−O(7)	112.7(2)
O(2)−As(1)−O(3)	116.1(2)	O(5)−As(2)−O(6)	112.2(3)
O(2)−As(1)−O(4)	103.7(2)	O(5)−As(2)−O(7)	118.5(3)
O(3)−As(1)−O(4)	103.3(2)	O(6)−As(2)−O(7)	108.3(3)
O(8)−As(3)−O(9)	107.4(2)		
O(8)−As(3)−O(10)	113.8(2)	As(1)−O(4)−As(2)	125.9(3)
O(8)−As(3)−O(11)	107.6(2)	As(1)−O(1)−Zn(1)	124.3(3)
O(9)−As(3)−O(11)	109.9(2)	O(9)−As(3)−O(10)	110.8(2)
O(10)−As(3)−O(11)	107.4(2)	Zn(2)−O(8)−Zn(2)[i]	100.2(2)
		Zn(1)−O(11)[e]−Zn(2)	118.9(2)
O(6)−H···O(5)[h]	117.9		

[a] Symmetry codes: (a) $x, -3/2 - y, 1/2 + z$; (b) $x, -1/2 - y, 1/2 + z$; (c) $2 - x, -1 - y, 1 - z$; (d) $2 - x, 1/2 + y, 1/2 - z$; (e) $1 - x, -1/2 + y, 1/2 - z$; (f) $1 - x, 1/2 + y, 1/2 - z$; (g) $1 - x, -y, 1 - z$; (h) $2 - x, -1/2 + y, 1/2 - z$; (i) $1 - x, -1 + y, 1 - z$.

Experimental Section

Synthesis. Hydrothermal reactions were performed in gold ampules contained in a Leco Tem-Pres autoclave. Colorless chunk crystals of $BaZn_2(HAs_2O_7)AsO_4$ were obtained from starting reagents of analytical grade or better: $Ba(OH)_2 \cdot 8H_2O$ (0.0221 g, 0.07 mmol), ZnO (0.0056 g, 0.07 mmol), 4.62 M H_3AsO_4 (0.3 mL, 1.386 mmol), and H_2O (0.1 mL) were sealed in a gold ampule (4.5 cm × 0.5 cm inside diameter) and heated at 550 °C and an estimated pressure of 33 300 psi for 12 h. The autoclave was cooled at 5 °C/h to 250 °C and quenched to room temperature by removing the autoclave from the furnace. The product was filtered off, washed with water, rinsed with ethanol, and dried in a desiccator at ambient temperature. The product contained colorless chunk crystals in the size of 0.15 mm or larger. A suitable crystal was selected and its structure determined by single-crystal X-ray diffraction (*vide infra*). The X-ray powder pattern of the reaction product compared well with that calculated from the single-crystal data.

Thermogravimetric analysis (TGA) was carried out using a DuPont 2200 thermal analyzer system in the temperature range 25−950 °C. The experiment was performed on a powder sample of selected single crystals of $BaZn_2(HAs_2O_7)AsO_4$ in air with a heating rate of 5 °C min^{-1}. Infrared absorption spectrum of $BaZn_2(HAs_2O_7)AsO_4$ was recorded with a Perkin-Elmer 882 spectrometer (4000−500 cm^{-1}; KBr disk).

Single-Crystal X-ray Structure Analysis. A crystal of dimensions 0.15 × 0.20 × 0.20 mm for $BaZn_2(HAs_2O_7)AsO_4$ was selected for indexing and intensity data collection on a Siemens Smart-CCD diffractometer equipped with a normal focus, 3 kW sealed-tube X-ray source ($\lambda = 0.710\ 73$ Å). Intensity data were collected in 1271 frames with increasing ω (width of 0.3° per frame). Unit cell dimensions were determined by a least-squares fit of 3002 reflections with $5 < 2\theta < 50°$. Of the 4538 reflections collected ($2\theta_{max} = 53.1°$), 1539 unique reflections ($R_{int} = 0.036$) were considered observed ($I > 3\sigma(I)$) after *Lp* and absorption corrections. The absorption correction was based on 3278 symmetry-equivalent reflections using the XPREP program[9] ($T_{min}/T_{max} = 0.479/0.969$). On the basis of systematic absences and statistics of intensity distribution, the space group was determined to be $P2_1/c$. The structure was solved by direct methods: the barium, zinc, and arsenic atoms were first located, and all the oxygen atoms were found in a difference Fourier map. Bond-valence calculations[10]

(9) Sheldrick, G. M. SHELXTL PC, Version 5, Siemens Analytical X-ray Instrument, Madison, WI, 1994.

Table 4. Motif of Mutual Adjunction, Coordination Number (CN), and Bond-Valence Sums (∑s) for $BaZn_2(HAs_2O_7)AsO_4$

	O(1)	O(2)	O(3)	O(4)	O(5)	O(6)	O(7)	O(8)	O(9)	O(10)	O(11)	CN	∑s
Ba	1/1	1/1	1/1		1/1	1/1	2/2		1/1	1/1		9	2.25
Zn(1)	1/1		1/1		1/1				1/1		1/1	5	2.01
Zn(2)		1/1						2/2		1/1	1/1	5	1.99
As(1)	1/1	1/1	1/1	1/1								4	5.07
As(2)				1/1	1/1	1/1	1/1					4	4.89
As(3)								1/1	1/1	1/1	1/1	4	4.85
H						1/1						1	1.16
CN	3	3	3	2	3	3	3	3	3	3	3		

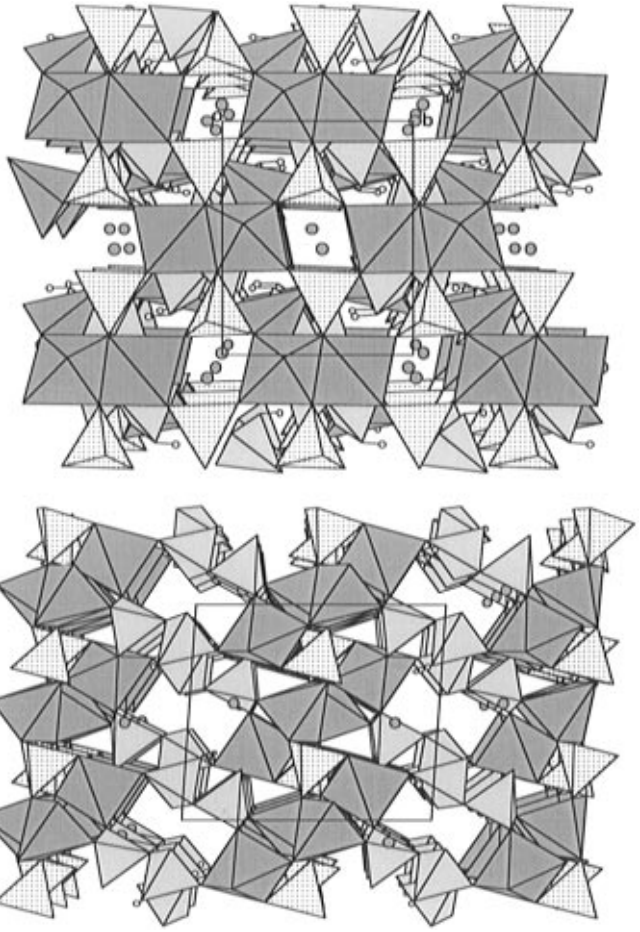

Figure 1. Perspective views of the $BaZn_2(HAs_2O_7)AsO_4$ structure along (a, top) the *a* axis and (b, bottom) the *b* axis. The structure may be viewed as stacking of $^2_\infty[Zn_2AsO_4^+]$ sheets and $^2_\infty[BaHAs_2O_7^-]$ layers along *a*. In these representations the corners of polyhedra are O atoms and the Zn and As atoms are at the center of each square pyramid and tetrahedron, respectively. The dark stippled polyhedra represent ZnO_5, the dotted tetrahedra AsO_4, the light stippled tetrahedra AsO_4 of the HAs_2O_7 groups, the stippled circles Ba, and the small open circles H.

indicated that O(6) was considerably undersaturated and all other oxygen atoms had values close to 2. One hydrogen atom must be included to balance charge. The valence sum of 1.25 for O(6) suggests that it is a hydroxyl oxygen. The hydrogen atom was located from a difference Fourier map calculated at the final stage of structure analysis. The final cycles of refinement, including the atomic coordinates and anisotropic thermal parameters for all non-hydrogen atoms and fixed atomic coordinates and isotropic thermal parameter for the H atom, converged at $R = 0.0244$ and $R_w = 0.0297$. In the final difference map the deepest hole was -0.88 e Å^{-3} and the highest peak 0.93 e Å^{-3}. Corrections for secondary extinction and anomalous dispersion were applied. Neutral-atom scattering factors were used. Structure solution and least-squares refinements were performed on a DEC VAX 4000/90 workstation using the SHELXTL-Plus programs.[11]

(10) Brown, I. D.; Altrmatt, D. *Acta Crystallogr.* **1985**, *B41*, 244.

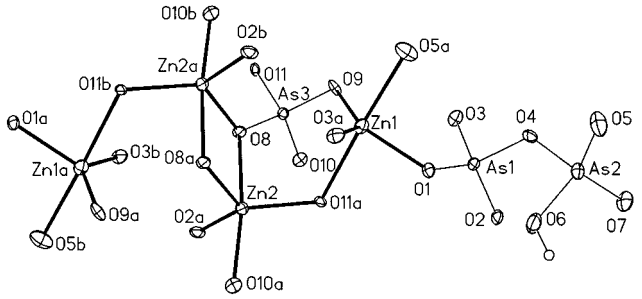

Figure 2. Part of the structure showing the Zn_4O_{16} cluster unit with atomic labeling. Thermal ellipsoids are shown at the 55% probability level.

Results and Discussion

The crystallographic data are listed in Table 1, atomic coordinates and thermal parameters in Table 2, selected bond lengths and bond angles in Table 3, and linkage motif and bond-valence sums in Table 4. The Zn and As atoms are five- and four-coordinated, respectively. The coordination number of the Ba atom was determined on the basis of the maximum gap in the Ba−O distances ranked in increasing order. The maximum cation−oxygen distance, L_{max}, according to Donnay and Allmann,[12] was also considered. Therefore, Ba is coordinated by nine oxygen atoms with the tenth Ba−O distance at 3.660 Å. The valence sum for Ba is saturated, indicating that the cations are tightly bound to the anionic network.

Views of the unit cell of $BaZn_2(HAs_2O_7)AsO_4$ are presented in Figure 1, and the characteristic part is illustrated in Figure 2. An edge-sharing dimer of square pyramids is formed between two inversion center-related Zn(2) pyramids. The dimer is further corner-shared with two Zn(1) pyramids resulting a tetrameric cluster unit of Zn_4O_{16}. As shown in Figure 3a, the tetramers are united in the *bc* plane by monoarsenate groups to form an infinite sheet $^2_\infty[Zn_2AsO_4]$ with a positive charge. Within a sheet, each cluster unit makes six Zn(2)−O−As(3) bonds and two Zn(1)−O−As(3) bonds to six $As(3)O_4$ tetrahedra. The apices of the two Zn(2) pyramids, O(2) and O(2a), are pointing to opposite directions, one to $+a$ and the other to $-a$. Two vertices of the Zn(1) pyramids, O(1) and O(5a), also cling to the *a*-axis direction. These four oxygens are bridging atoms between Zn and the As of HAs_2O_7 groups. As a consequence, $^2_\infty[Zn_2AsO_4]$ sheets are connected by diarsenate tetrahedra along the *a* axis to form a 3-D framework with intersecting tunnels. The tunnels which are parallel to the *a* axis show small tetragonal windows at the opening. The tunnels which are running parallel to the *b* axis show rather large windows, each is formed by two $Zn(1)O_5$ pyramids and four AsO_4 tetrahedra of the HAs_2O_7 groups. Barium cations are located at the intersections of these perpendicular sets of tunnels.

It is noted that, between two $^2_\infty[Zn_2AsO_4]$ sheets, HAs_2O_7 units and barium cations form a layer as well. As depicted

(11) Sheldrick, G. M. SHELXTL-Plus Crystallographic System, release 4.21, Siemens Analytical X-ray Instrument, Madison, WI, 1991.
(12) Donnay, G.; Allmann, R. *Am. Mineral.* **1970**, *55*, 1003.

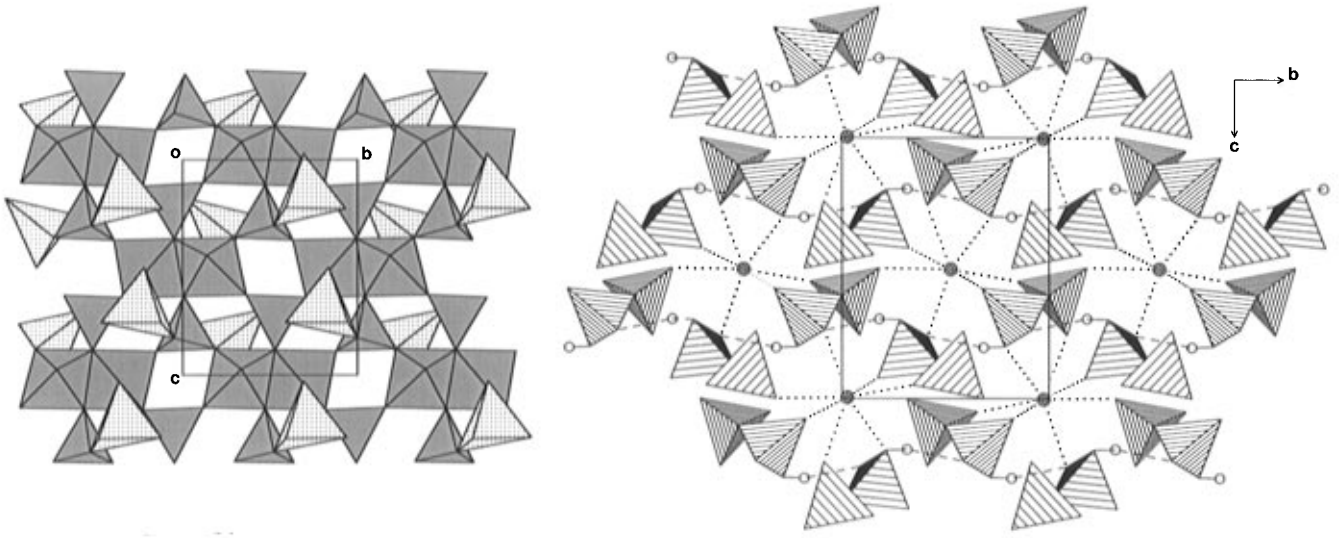

Figure 3. Two-dimensional sheets in the $BaZn_2(HAs_2O_7)AsO_4$ structure. (a) Left: Section of the $^2_\infty[Zn_2AsO_4]$ sheet. The stippled polyhedra represent ZnO_5, and the dotted tetrahedra, AsO_4. (b) Right: Section of the $^2_\infty[BaHAs_2O_7]$ layer. The striped polyhedra represent As_2O_7, the cross-hatched circles Ba, the small open circles H, the dashed lines H-bonds, and the dotted lines Ba−O bonds.

in Figure 3b, HAs_2O_7 groups are H-bonded into infinite $^1_\infty[HAs_2O_7]$ chains parallel to the [010] direction. $^1_\infty[HAs_2O_7]$ chains are further connected by barium cations to form a $^2_\infty[BaHAs_2O_7]$ layer with a negative charge. The structure of $BaZn_2(HAs_2O_7)AsO_4$ may be alternatively viewed as stacking of $^2_\infty[Zn_2AsO_4]$ sheets and $^2_\infty[BaHAs_2O_7]$ layers along *a*. The large tunnels which are perpendicular to the stacking direction are located within the $^2_\infty[BaHAs_2O_7]$ layers. There are actually large cavities within these anionic layers. Each cavity is surrounded by twelve tetrahedra from two adjacent $^1_\infty[HAs_2O_7]$ chains. Barium cations only occupy a portion of the large cavities.

One of the interesting features of $BaZn_2(HAs_2O_7)AsO_4$ is the existence of Zn_4O_{16} cluster units. This tetrameric unit, which consists of alternate corner- and edge-shared ZnO_5 square pyramids, is found for the first time in the Zn/X/O lattices (X = P, As). There are two unique zinc atoms in the cluster unit, Zn(1) and Zn(2). The $Zn(2)O_5$ unit is more distorted from an ideal square pyramid than the $Zn(1)O_5$ unit as shown by its deviated bond angles, e.g., 79.8 and 171.1° vs 85.1 and 174.9° (Table 3). The larger deviation is probably due to edge-sharing between the two Zn(2) pyramids. The bond angle at the bridging atom O(8), 100.2°, is slightly greater than those found in the other two dimer-containing phosphates, $Zn_2VO(PO_4)_2$[6] (96.3°) and α-$CaZn_2(PO_4)_2$[5] (99.7°). Further analysis on the dimer shows that the Zn(2)−Zn(2) distance is significantly longer than that between the two polyhedra centers, 3.22 vs 2.95 Å, whereas it is shorter in discrete dimers, 2.98 vs 3.10 Å in $Zn_2VO(PO_4)_2$ and 3.02 vs 3.40 Å in α-$CaZn_2(PO_4)_2$. The mutual repulsion of the Zn(2) atoms also reflects on the resulting bond angles at bridging atoms, 100.2 vs 95.2°(if calculated on the basis of the polyhedra centers). Data for $Zn_2VO(PO_4)_2$ and α-$CaZn_2(PO_4)_2$ are 96.3 vs 99.3° and 99.7 vs 106.3°, respectively. It is apparent that the addition of corner-shared Zn(1) pyramids to the Zn(2) dimers counterbalance the electrostatic forces among the four central atoms in the Zn_4O_{16} cluster unit. Therefore, instead of coming closer, edge-shared Zn(2) centers are dragged away from each other. The repulsion is considered moderate when compared with another dimer-containing compound, $Zn_2Cu(AsO_4)_2$.[7] In this structure the two ZnO_5 pyramids in a dimer, which is not discrete in a sense, are severely distorted and the distance between them is deviated from the polyhedra centers by ∼0.66 Å. On the other hand, the Zn(1) centers in the Zn_4O_{16} cluster units are coming slightly closer to the Zn(2) centers, 3.60 vs 3.64 Å. These distances are comparable with those (3.62 vs 3.63 Å) of the structure of $Zn_2(AsO_4)_2OH$[13] in which similar Zn−O−Zn linkage between corner- and edge-shared polyhedra chains are present.

Another interesting feature is the hydrogen diarsenate unit, HAs_2O_7, in the structure. A few phosphates such as $CaNH_4HP_2O_7$,[14] $K_2H_2P_2O_7$,[15] and $Cs_2HP_2O_7$[16] contain hydrogen diphosphate groups. In contrast, compounds containing HAs_2O_7 groups have not been documented. In the title structure, the two AsO_4 tetrahedra in HAs_2O_7 are in a staggered configuration with an As−O−As angle of 125.9°, comparable to the angle 124.7° of another barium-bonded copper diarsenate, $BaCuAs_2O_7$.[17] The H-bonds (Table 3) between HAs_2O_7 groups are weak as compared with those in hydrogen diphosphate anions. The HAs_2O_7 units are tightly bonded to the barium cations within the $^2_\infty[BaHAs_2O_7]$ layer as the average Ba−O distance is 2.81 Å, which is shorter than 2.89 Å, the sum of Shannon crystal radii of nine-coordinated Ba^{2+} (1.61 Å) and O^{2-} (1.28 Å).[18]

The infrared absorption spectrum of $BaZn_2(HAs_2O_7)AsO_4$ showed a broad band near 3390 cm^{-1} due to typical O−H stretching in a hydrogen-bonded environment. A sharp band at 1140 cm^{-1} is probably the hydrogen diarsenate As−OH mode.[19] The bands corresponding to symmetric and asymmetric As−O−As vibration modes of HAs_2O_7 are centered at 560 and 769 cm^{-1}, respectively. In addition, the As−O stretching frequencies associated with the $[AsO_4]$ can be observed at 825, 852, 875, and 927 cm^{-1}. These values are consistent with the characteristic bands for $Na_4As_2O_7$.[19]

A three-stage weight-loss scheme was observed on the TGA curve (Figure 4). The first stage, which occurs from 250 to ≈530 °C, is attributed to the loss of a half water molecule. The second stage occurs between temperatures of ≈530 and 620 °C, which is due to the release of $^1/_4$ O_2 from the above product.

(13) Hill, R. J. *Am. Mineral.* **1976**, *61*, 979.
(14) Mathew, M.; Schroeder, L. W. *Acta Crystallogr.* **1977**, *B33*, 3025.
(15) Larbot, P. A.; Durand, J.; Norbert, A.; Cot, L. *Acta Crystallogr.* **1983**, *C39*, 6.
(16) Averbuch-Pouchot, M. T.; Durif, A. *Eur. J. Solid State Inorg. Chem.* **1993**, *30*, 1153.
(17) Chen, T. C.; Wang, S. L. *J. Solid State Chem.* **1996**, *122*, 36.
(18) Shannon, R. D. *Acta Crystallogr.* **1976**, *A32*, 751.
(19) Nakamoto, K. In *Infrared and Raman Spectra of Inorganic and Coordination Compounds*, 4th ed.; Wiley: New York, 1986.

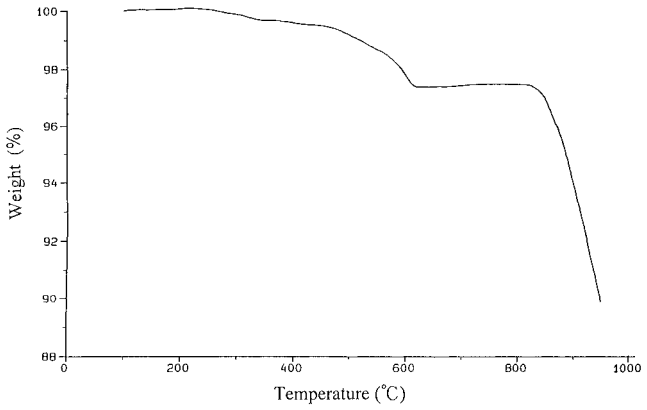

Figure 4. Thermogravimetric analysis of $BaZn_2(HAs_2O_7)AsO_4$.

The evolvement of oxygens is not resolved well from the first step as shown on the TG curve. Nonetheless, the observed total weight loss (2.58%) of the first two stages can be compared with the calculated value of 2.54% based on the above interpretation. Furthermore, there is a third sharp fall in weight loss beyond ≈820 °C which suggests vaporization of As_2O_3 from the decomposition products. The kind of decomposition corresponding to the last two stages was observed in a vanadyl arsenate, $BaVOAsO_4(HAsO_4)\cdot H_2O$.[1]

In conclusion, a novel barium zinc hydrogen diarsenate, $BaZn_2(HAs_2O_7)AsO_4$, has been synthesized under hydrothermal conditions. This compound adopts a new structure type which is featured in the unusual tetrameric Zn_4O_{16} units and HAs_2O_7 groups. The barium cations are located in large cavities surrounded by HAs_2O_7 anions. The structure also shows a novel feature where two-dimensional zinc monoarsenate sheets are intergrown with the barium salt of hydrogen diarsenate.

Acknowledgment. We thank the National Science Council of the Republic of China for support of this work (Grant NSC85-2113-M-007-005).

Supporting Information Available: Tables giving detailed crystal data, bond distances and angles, and anisotropic thermal parameters for $BaZn_2(HAs_2O_7)AsO_4$ (4 pages). Ordering information is given on any current masthead page.

IC951655H